BASELINE SYSTEM DESIGN AND PROTOTYPING FOR THE ITER HIGH-FREQUENCY MAGNETIC DIAGNOSTICS SET

D.Testa, R.Chavan, J.Guterl, J.B.Lister, J-M.Moret, A.Perez, F.Sanchez, B.Schaller, G.Tonetti, M.Toussaint
Ecole Polytechnique Fédérale de Lausanne (EPFL)
Centre de Recherches en Physique des Plasmas
Association EURATOM-Confédération Suisse
CH-1015 Lausanne, Switzerland
e-mail address of contact author: duccio.testa@epfl.ch

A.Encheva, G.Vayakis, C.Walker
ITER organization
F-13108 Saint-Paul-lez-Durance, France

Y.Fournier, T.Maeder
Laboratoire de Production Microtechnique (LPM), EPFL
CH-1015 Lausanne, Switzerland

H.Carfantan
Laboratoire d'Astrophysique de Toulouse-Tarbes (LATT)
Université de Toulouse - CNRS
F-31400 Toulouse, France

This paper reports the mechanical and electrical tests performed for the prototyping of the ITER high-frequency magnetic sensor and the analysis of the measurement performance of this diagnostic. The current design for the sensor is not suitable for manufacturing for ITER due to the high likelihood of breakages of the un-guided tungsten wire during the winding. A number of alternative designs and manufacturing processes have been investigated, with the Low Temperature Co-fired Ceramic technology giving the best results. The measurement performance of the baseline system design for the high-frequency magnetic diagnostic cannot meet the intended ITER requirements due to its intrinsic spatial periodicities.

Keywords: ITER, high-frequency magnetic diagnostic, LTCC

I. INTRODUCTION

The current design for the high-frequency (HF) magnetic sensor for ITER is a conventional, Mirnov-type, pick-up coil, i.e. a metallic wire wound around a ceramic support, with an effective area $(NA)_{EFF} \approx 0.1 m^2$. Figure1 shows this design.

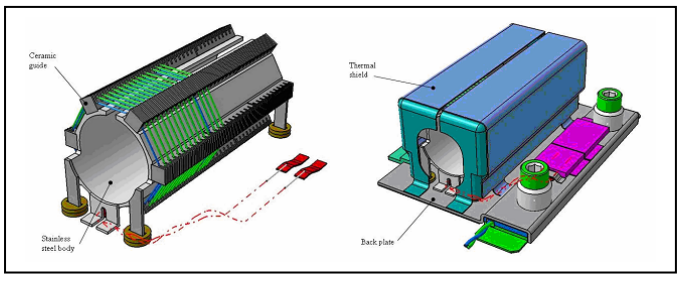

Figure 1. *ITER original pick-up coil assembly: the detailed view (left), showing the stainless steel body, the ceramic grooving used to guide the wire and the winding pack, and the overall assembly (right), showing the thermal shield, the back plate attachment and coil-cable connector unit.*

The ITER HF magnetic sensor is intended to be made using a tungsten wire with 33 turns each on 2 separate layers, wound over a hollow hexagonal ceramic body made of individual wire spacers, without guiding grooves. A hollow stainless steel (SS) core mechanically supports the spacers and improves thermal conduction. A thermal shield is added, and the coil is then fixed onto a supporting metal plate (the "back" plate) that allows thermal and electrical contact with the vacuum vessel.

The ITER HF magnetic diagnostic system is intended to provide measurements of magneto-hydrodynamic instabilities with magnitude as low as $|\delta B| \sim 10^{-4} G$ and up to frequencies >300kHz, with toroidal (n) and poloidal (m) mode numbers up to |n|=30 and |m|=60 [1]. Figure2 shows the nominal baseline design for this system, which is built around 2 main arrays for toroidal and 6 main arrays for poloidal mode number detection.

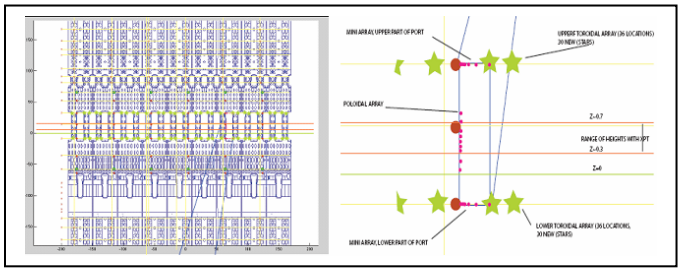

Figure 2. *The proposed layout for the ITER HF magnetic diagnostic system (left), for n- (green stars) and m- (red dots) number detection; yellow dots with green edges indicates those sensors whose position clashes with that of the ELM assemblies; on the right, the proposed ITER implementation for the high-resolution toroidal and poloidal arrays (small red dots) to be located on the horizontal and vertical edges of some of the equatorial ports.*

The 2 arrays for toroidal mode number detection (indicated by green stars in fig2, which surround the equatorial ports) are made with 2x18 equi-spaced sensors each and are positioned at two different heights with respect to the geometrical centre of the machine, using the corners of each equatorial port on the low field side wall. Hence, these arrays have by construction a

20deg/18-fold periodicity, giving an intrinsic Nyquist number n=9 on each of the two periodic sub-assemblies, whereas the ITER measurement requirements specify accurate detection of modes up to |n|=30. This system design has another weakness, namely the absence of sensors for n-number detection on the high field side of the ITER vacuum vessel. This does not allow distinction between ballooning and anti-ballooning instabilities.

The poloidal mode number detection system is built around 18 un-evenly spaced sensors located on six machine sectors, covering the entire poloidal cross-section but for the divertor region. The recent addition of the in-vessel active ELM coil assemblies to the ITER design has reduced the six m-number arrays to 16 sensors each, as the position of two of the sensors clashes with that of the ELM assemblies.

The toroidal (and poloidal) mode number detection system can be improved in the ITER original design layout, with initial provisions already being made for this, by adding a high-resolution array on the horizontal (vertical) edge of some of the equatorial ports on the low-field side. This will in principle remove the n=9 toroidal Nyquist value by adding un-evenly spaced sensors to the two original periodic sub-assemblies.

II. Prototyping of the ITER HF magnetic sensor

A coupled electro-magnetic, structural and thermal analysis was first performed on the original design for the HF sensor to find which of its components might be weaker [2]. We found that differences in the thermal expansion of the various parts of the sensor produce stress in the wire. Depending on the wire initial pre-load, this can break the wire or the ceramic supports. Hence, the mechanical characteristics of the prototypes were analyzed with particular attention to the assembly process for the winding pack, by using different types of guiding grooves on the ceramic support and materials for the wire.

The conventional prototypes were produced at a cost of ~50USD per unit using the so-called "Rapid Prototyping" (RP) technology [3] to manufacture the support for the winding pack instead of the ceramic material envisaged in the ITER design. Hence, the thermal and out-gassing properties of the various prototypes were not analyzed as these were not going to be representative of the "as built" pick-up coil. The electrical properties were fully analyzed via direct measurements of the coil's transfer function and modeling of the equivalent circuit. One essential feature of the ITER original design for the HF pick-up coil is the SS core, used to provide mechanical support and thermal conduction for the ceramic body and the winding pack. This SS core changes the electrical characteristic of the HF coil because it acts intuitively as a capacitively-loaded one-turn secondary of a transformer, the primary being the winding pack itself. The thermal shield was also added for the electrical characterization of the different prototypes, but their electrical properties were not affected.

In addition to the original ITER design for the HF coil, two further prototypes for the body of the coil were designed, so as to include some improvements for the guiding grooves [2]. In our "first modified version" the wire is guided during the changing of turns using straight guiding grooves on the ceramic body. The problem with this solution is that there is now a collision between the grooves of the two layers, creating a narrow edge. The collision between the two layers increases the brittleness in the groove's walls. Hence, we designed a "second modified version" to tackle this problem, using passing holes as guiding grooves. The wire is still guided along the turn changes and across the superposed layers, but the grooves do not enter in collision as now the wire has to pass into holes for the turn changes, thus separating the first from the second layer. The walls and edges of the grooves are stronger, but now the wire is more difficult to wind, as it has to be guided through a hole at each turn change. Winding tests were performed using a copper and a tungsten (the currently foreseen material) wire on each prototype version to test the robustness of the winding process. Figure3 shows some of the different as-built prototypes.

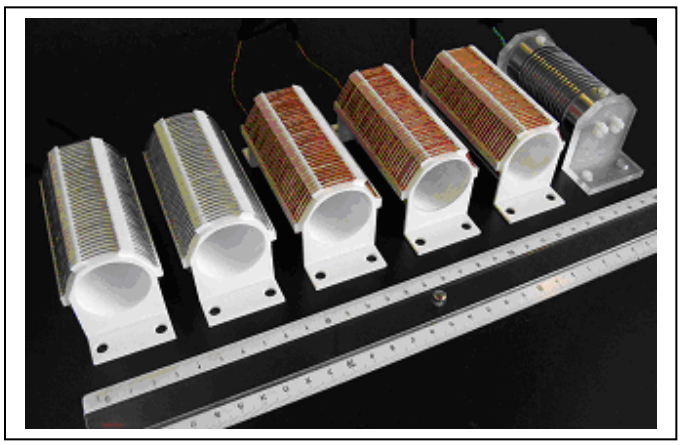

Figure 3. *From left to right, five examples of the as-built prototypes for the ITER HF pick-up coil of conventional, Mirnov-type design; the sixth, rightmost coil was made in SS 316 using the laser-cutting technique.*

Our test program has demonstrated that the three winding processes envisaged for the ITER original design for the HF pick-up coil are not adequate. This operation is difficult to carry out and also generates tension in the support parts and in the wire, which in turns causes a deformation in the shape of the coil. Another problem with the conventionally wound coil is the difficulty to manufacture a ceramic body of sufficient strength. Finally, the tungsten wire currently foreseen for ITER can easily be broken during the many operations necessary to assemble the winding pack because. Hence, this material is not acceptable for ITER and further winding tests will need to be performed with other wires, such as Glidcop or molybdenum.

An alternative solution for the conventional HF coil would be to have a metallic "winding" pack made of one single part. With this technique, we can completely avoid manufacturing the complicated ceramic body and eliminate all the difficulties associated to the winding process itself. This alternative design has been realized by laser-cutting an equivalent winding pack from a hollow metallic tube, a process which has been easily performed with current CAD processes [2]. This prototype is shown at the rightmost end of fig3, as mounted on a Plexiglas support, which is used to maintain the coil in its correct shape.

Another approach to reduce manufacturing risks on the ITER HF magnetic diagnostic is to develop a prototyping program with different designs and technologies. The Low Temperature Co-fired Ceramic (LTCC) technology is a good start, as it is

an industry standard widely used for high temperature/vacuum applications. Its predecessor, the HTCC (High-Temperature) standard, has been used for manufacturing the low-frequency pick-up coils on LHD [4]. Some tests were also performed for the equilibrium sensors for ITER [5]. An LTTC sensor is built up from ~100-400μm thin ceramic tapes, onto which a metallic ink is screen printed to form windings and to ensure interlayer electrical contact through via holes. The tapes are then stacked on top of each other, possibly intercalated with additional tapes carrying no winding planes to decrease interlayer capacitance, laminated and fired in air at ~875°C. Various prototypes for this magnetic sensor have been realized in-house by changing the number of and the separation between the ceramic layers, and the number of turns on each layer, so as to assess the electrical properties of the sensors [6]. Figure4 shows the printing screen and some of the as-built LTCC sensors.

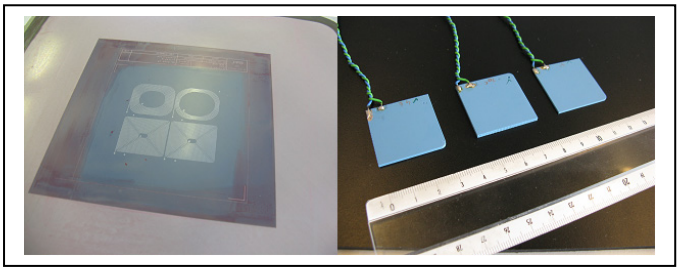

Figure 4. *On the left, design of a set of LTCC sensors during the serigraphic printing process; on the right, three as built LTCC sensors: note their small size compared to the Mirnov-type conventional pick-up coils shown in fig3.*

The great advantage of the LTCC technology resides in its very small and compact size, which makes it possible to design and manufacture a 3D magnetic sensor using a fraction of the volume needed for 3x 1D conventional pick-up coils. The main drawback of this solution is related to the metallic ink used to print the circuit, as currently manufacturing processes are only available for gold and silver, whereas such inks may have to be avoided in ITER because of the risk of transmutation under heavy neutron and radiation fluxes. It is currently foreseen to further develop the LTCC technology so as to assess the use of the more ITER-relevant palladium and platinum inks.

The electrical characteristics of the prototype HF magnetic sensors have been extracted from the measurement of the coil impedance following the technique described in [7]. For the measurement of the effective and stray area, an Helmholtz coil assembly was used. When considering the ITER measurement requirements for the HF magnetic diagnostic set, the estimated length (>50m) and the electrical specifications for the signal cables and the data acquisition modules, it is clear that the HF magnetic sensor must have a self resonance frequency >5MHz with a quality factor better than 5%. All the as-built prototypes have been found to meet concurrently these requirements when suitable design choices are made [2, 6].

III. Analysis of the Measurement Performance of the ITER HF Magnetic Diagnostic

We have performed the baseline analysis and optimization of the ITER HF magnetic diagnostic system using a new approach based on the "*sparse representation of the signal spectrum*", the so-called *Sparse Spectrum* algorithm. This technique has been originally implemented in the *SparSpec* code for the analysis of astronomical data [8]. The application of this method to real and simulated JET data [9] has clearly demonstrated its superiority to other analysis and optimization methods in several respects. The *Sparse Spectrum* algorithm has been applied to a model dataset of input modes for various implementations of the ITER HF magnetic sensor geometry for n(m)-number detection. The ITER measurement requirements and the expected measurements' errors and tolerances are explicitly considered in this algorithm to define the *correct* and the *wrong* detection of the modes. We have then defined four complementary tests to assess the measurement performance of any given magnetic sensor geometry [10].

First, we use an input dataset made only of white Gaussian noise of known variance, and we determine the 95% and 99% confidence level for not detecting any mode. This allows us to assess if one particular sensor arrangement is more prone than the others to wrongly take white noise for high-n(m) modes.

Second, we consider the statistics of correctly recognizing the given input real modes, to which white Gaussian noise of known variance is added, vs. the occurrence of "false alarms", i.e. modes being detected but which are not in the input dataset. The sensor arrangements giving the higher number of correctly detected modes and the lower values of false alarms are then the best choices for actual in-vessel installation.

Third, we consider the resilience of the selected geometry against the loss of sensors through faults. A measure for this is given by the relative error on the fitting of the input mode spectrum for the cases of "*all vs. not-all*" sensors being used. It is clear that, once the fitting error using all sensors is accepted as giving good measurements, the lower the relative error over the permutations of lost sensors and input spectrum variations, the more resilient is that geometry against the loss of sensors.

Fourth, we consider the position of each individual sensor as not absolutely fixed, but that there is a given volume where the sensor has to be located. This adds a new free parameter, i.e. a tolerance on the nominal position of each sensor as given by in-vessel surveys, which are expected to be accurate within ±0.5deg. When considering the manufacturing and installation tolerances for the ITER in-vessel components, the calibration errors and the uncertainties in the equilibrium reconstruction, the calculated position of each sensor is in fact expected to be correct only to ±3deg. Given an input spectrum to be detected, we can then artificially move the initial position of each sensor within this ±3deg tolerance to achieve the "best" measurement performance, which has then no consequence for the in-vessel installation. Only when the optimization algorithm suggests a larger displacement of the sensors, we must then change their position. Hence, the more the sensors are displaced to optimize the measurement performance, the less robust is the initial non-optimized geometry against variation in the input spectra.

Starting from the nominal layout of the ITER HF magnetic diagnostic set, we have developed different implementations of this system. The more robust sensor geometry is the un-evenly spaced one, i.e. one without periodicity in the sensors' spacing. For the foreseeable input spectra, a truly randomly distributed geometry is the more resilient to the loss of faulty sensors, and

also requires less displacement in the position of each sensor to optimize its measurement performance. These geometries are much less sensitive to false alarms caused by background noise in the input spectrum, as geometries based on un-evenly spaced sensors allow reducing the total number of sensors with respect to geometries with periodicities in the sensors' spacing. On the other hand, a geometry made up of equi-spaced sub-assemblies presents the lowest resilience to the loss of sensors, even if the initial number of sensors is larger than that needed to obtain the required spatial Nyquist number. This can only be improved by breaking the original spatial symmetries adding (2-3 for n-numbers, but only 1 is possible for m-numbers) high-resolution arrays in well-apart equatorial ports, each array being made of 3-7 un-evenly spaced sensors. However, adding such arrays to equi-spaced geometries considerably increases the total number of sensors and associated in-vessel services that need to be installed. Finally, our simulations indicate that a separation <3deg between adjacent sensors is not necessarily beneficial, even for high-n(m) detection, as random phase shifts due to background noise mask the "true" phase shifts for the closest sensors, which in turns makes it more difficult to detect high-n(m) modes with a sufficiently high confidence level.

The nominal geometry for toroidal mode number analysis (2 sub-assemblies of 18 sensors each, located at the corners of each equatorial port), does not satisfy the criteria for robustness in the measurement performance due to its spatial periodicity. The addition of high-resolution arrays inside the equatorial ports is beneficial for this baseline geometry only provided at least 3 well-separated ports are used, with 3-7 additional, un-evenly distributed sensors in each port. This therefore makes a total of >45 sensors in each array used for n-number detection. This number does not compare well with the ~30-35 un-evenly spaced sensors which represent the best geometry to satisfy the ITER measurement requirements for toroidal mode numbers.

The nominal geometry for poloidal mode number detection (16 sensors, excluding those whose position clashes with that of the ELM assemblies and blacking-out the divertor region) performs better than its n-number counterpart, but still does not satisfy the ITER measurement requirements. Adding one high resolution array with 5-7 sensors in the equatorial port slightly improves this situation. However, only a randomly distributed geometry with 25-30 sensors in total, plus one high-resolution port array, satisfies completely the requirements for robustness and resilience of the measurement performance.

These analyses consider areas that cannot be used to install HF magnetic sensors only in reference to the divertor region, the location of the new ELM assemblies and upper/lower ports. Additional engineering constraints, such as cabling access and in-vessel structures capable of inducing eddy (image) currents affecting the frequency response of the HF magnetic sensors, will need to be integrated in future analyses to be able to decide on the final geometry for the HF magnetic set. A compromise will have to be made between in-vessel installation constraints and achieving the required measurement performance with high robustness. Hence, the main criteria to satisfy the ITER measurement requirements for the HF magnetic diagnostic will be the availability of space in at least 3 well apart equatorial ports to install high-resolution, symmetry-breaking arrays of 5-7 sensors. This can be combined with the foreseen installation of the poloidal arrays in 6 machine sectors.

Taking into account all these considerations, an optimized outline design for the ITER HF magnetic diagnostic system for toroidal and poloidal mode numbers analysis is proposed [10]:

a) toroidal mode numbers (main measurement arrays): on the low-field side, 2 arrays on the horizontal side of the equatorial ports, each array with 20 un-evenly spaced sensors plus 6x5 high resolution arrays located in each one of the equatorial ports used by the poloidal HF magnetic sensor system;

b) toroidal mode numbers (anti-ballooning mode analysis, redundancy and backup via diversity of location): on both the low- and high-field side, 2 arrays of 25-30 un-evenly spaced sensors located between 45cm and 70cm above and below the centre of each equatorial port.

c) poloidal mode numbers: one array of 20-25 un-evenly spaced and 5-7 high resolution sensors in 6 ports in non equi-distant machine sectors, not covering the divertor region and the areas around the top of the vessel.

These geometries give a large redundancy in the toroidal and poloidal mode number measurements, and include in total 2x(20+30) (a) + 4x(25-30) (b) + 6x(25-30) (c) = 350-400 sensors for analysis of HF magneto-hydrodynamic instabilities in ITER. This is at least twice the number of ~170 HF magnetic sensors originally foreseen for ITER.

ACKNOWLEDGMENT

This work, supported by the European Communities under Contracts of Association, and by the national funding of the participating Associations, was partly carried out within the framework of the European Fusion Development Agreement, under Tasks TW4-TPDS-DIASUP, TW5-TPDS-DIASUP, TW6-TPDS-DIADES and TW6-TPDS-DIADEV. The views expressed in this publication are the sole responsibility of the authors and do not necessarily reflect the views of Fusion for Energy or the European Commission.

REFERENCES

[1] A.J.H.Donné et al., Nucl. Fusion **47** (2007), S337.

[2] D.Testa et al., "*Prototyping the ITER high frequency magnetic sensor using the conventional, Mirnov-type, pick-up coil*", unpublished.

[3] H.Li, X.Zeng, Journal of Mat. Proc. Tech. **184** (2007), 184.

[4] H.Takahashi, S.Sakakibara, Y.Kubota, and H.Yamada, Rev. Sci. Instrum. **72** (2001), 3249.

[5] G.Chitarin et al., "*Technology development for ITER in-vessel equilibrium magnetic sensors*", Fus. Eng. Des. (2009), in press.

[6] D.Testa et al., "*Prototyping the ITER high frequency magnetic sensor using the non-conventional LTCC technology*", unpublished.

[7] R.Heeter et al., Rev. Scient. Instrum. **71** (2000), 4092.

[8] S.Bourguignon, H.Carfantan, T.Böhm, Astronomy and Astrophysics **462** (2007), 379; see also http://www.ast.obs-mip.fr/softwares.

[9] A.Klein et al., Plasma Phys. Control. Fusion **50** (2008), 125005.

[10] D.Testa et al., "*Functional performance analysis and optimization for the high-frequency magnetic diagnostic system in ITER*", unpublished.